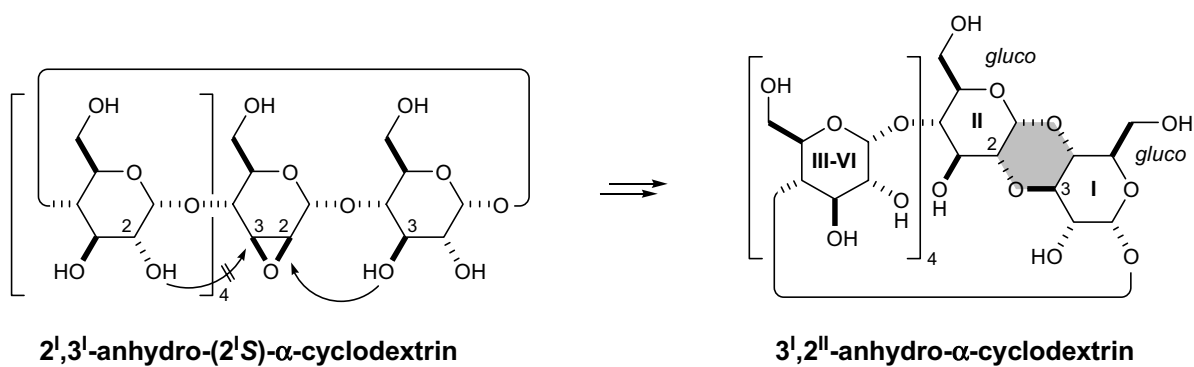


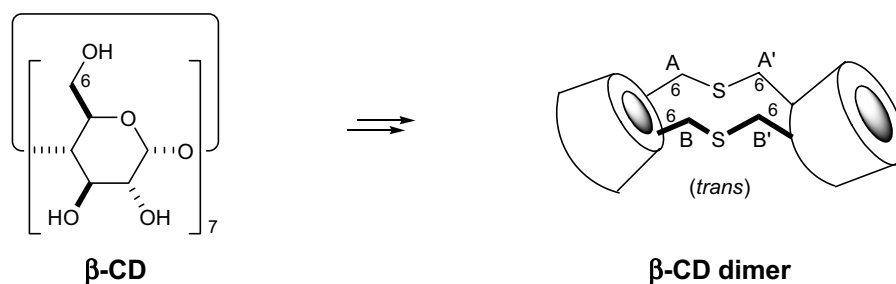
Chapter 7

Rigidified Bridged Cyclodextrins



Two Stereoisomeric 3',2''-Anhydro- α -cyclodextrins: A Molecular Dynamics and Crystallographic Study

S. Immel, K. Fujita, M. Fukudome, and M. Bolte,
Carbohydr. Res. **2001**, 336, 297-308.



The First Successful Crystallographic Characterization of a Cyclodextrin Dimer: Efficient Synthesis and Molecular Geometry of a Doubly Sulfur-bridged β -Cyclodextrin

D.-Q. Yuan, S. Immel, K. Koga, M. Yamaguchi, and K. Fujita,
Chem. Eur. J. **2003**, 9, 3501-3506.



Two stereoisomeric 3^I,2^{II}-anhydro- α -cyclodextrins: a molecular dynamics and crystallographic study[☆]

Stefan Immel,^{a,*} Kahee Fujita,^b Makoto Fukudome,^b Michael Bolte^{c,†}

^a*Institut für Organische Chemie, Technische Universität Darmstadt, Petersenstraße 22,
D-64287 Darmstadt, Germany*

^b*Faculty of Pharmaceutical Sciences, Nagasaki University, 1-14 Bunkyo-machi Nagasaki 852-8521, Japan*

^c*Institut für Organische Chemie, J.W. Goethe-Universität Frankfurt, Marie-Curie-Straße 11,
D-60439 Frankfurt (Main), Germany*

Received 10 August 2001; accepted 8 October 2001

Abstract

Regioselective epoxide ring opening of 2^I,3^I-(2^I*S*)-anhydro- α -cyclodextrin (**1**) through intramolecular attack of hydroxyl groups of neighboring glucose rings occurs in diequatorial fashion to yield 3^I,2^{II}-anhydro- α -cyclodextrin (**3**) with a rigid glucopyranose–dioxane–glucopyranose tricyclic ring system, the usual diaxial opening and the gluco/altro-configured stereoisomer **2** cannot be detected. Molecular dynamic simulations in water were used to analyze the conformations of **1–3** and the stereochemical implications of this reaction. Due to the contracted 2,3-OH side of the torus, **3** features an inverted conicity compared to the parent α -cyclodextrin. A crystallographic study on the bis-3:3 *n*-PrOH nonahydrate not only displays little variations between the solid-state and solution geometries of **3**, but also provides a molecular picture of a unique inclusion complex in which three *n*-propanol molecules are distributed in the cavity of a dimeric unit of **3** (monoclinic, space group *P*2₁, *a* = 14.257(1), *b* = 22.623(2), *c* = 16.644(1) Å, β = 104.82(1)°, all 19278 reflections with *I* > 2 σ (*I*) yield *R*(*F*) = 0.1017). © 2001 Elsevier Science Ltd. All rights reserved.

Keywords: 2^I,3^I-(2^I*S*)-Anhydro- α -cyclodextrin; 3^I,2^{II}-Anhydro- α -cyclodextrin; Molecular dynamics; Crystal structure; *n*-Propanol inclusion complex

1. Introduction

Cyclodextrin (CD) 2,3-*manno*-epoxides^{2–10} are highly useful intermediates in the course of chemical transformations of the backbone structure of these macrocycles.^{11,12} In general,

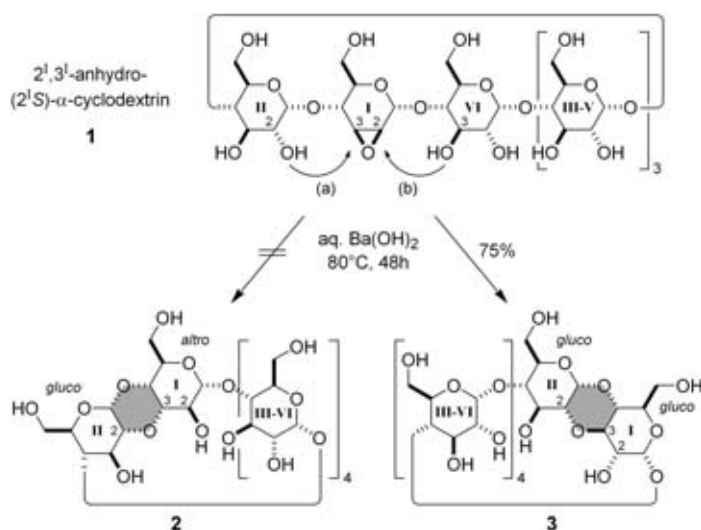
epoxide ring opening occurs highly selectively through nucleophilic attack in a trans-diaxial type fashion at C-3, offering versatile synthetic routes towards, e.g., per-3-deoxy-cyclomannans,¹³ mono-*altro*-CDs,^{14–16} di-*altro*-CDs,¹⁷ and cycloaltrans (α -, β -, and γ -‘cycloaltrin’),^{18–22} although the alternative diequatorial ring opening at C-2 has also been observed to occur to a lesser extent for various sulfur- and nitrogen-containing nucleophiles.²³ It therefore may be surmised, that intramolecular variations of this reaction proceed with similar stereo- and regioselectivity. In the case of 2^I,3^I-(2^I*S*)-anhydro- α -CD (**1**), the in-

[☆] Molecular modeling of saccharides, Part 30. For Part 29, see Ref. 1.

* Corresponding author. Tel.: +49-6151-165277; fax: +49-6151-166674.

E-mail address: lemmi@sugar.oc.chemie.tu-darmstadt.de (S. Immel).

[†] X-ray analysis, solution, and refinement.



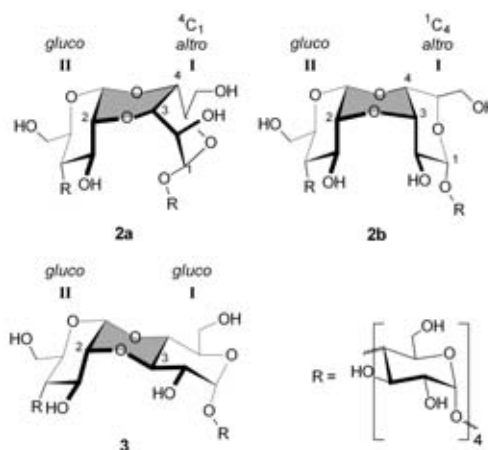
Scheme 1. Competing pathways (a) and (b) for the intramolecular ring opening of the mono-epoxide of α -cyclodextrin **1** through attack of neighboring hydroxyl groups (along pathway (b) the labeling of the sugar units changes).

tramolecular attack on the epoxide can involve either the 2^{II}-OH or 3^{VI}-OH group of the adjacent glucose residues (cf. Scheme 1). Along pathway (a), the trans-diaxial type opening leaves the pyranoid ring I with alto-configuration, whereas the alternative reaction path (b) generates a glucopyranoid ring I (diequatorial epoxide opening). Unexpectedly, the base-induced formation of the 1,4-dioxane ring exclusively proceeds via pathway (b), i.e. **1** \rightarrow **3**, the formation of **2** was not observed.²⁴

As an interpretation of this finding, it was brought forth that the trans-diaxial opening of the epoxide is sterically hindered by the macrocyclic structure of the CD derivative.²⁴ Although flexible CD derivatives or non-glucose cyclooligosaccharides²⁵ receive interest in mimicking the induced-fit type molecular recognition¹⁶ by enzymes,²⁶ a study on the binding ability of methyl orange towards a number of CDs with deformed cavities indicated that the higher homolog of **3**, i.e. 3^I,2^{II}-anhydro- β -CD (**4**) is the only candidate amongst the compounds studied to exhibit stronger binding (by about a factor of 2.8 at 10 °C) than β -CD itself.²⁷ In this context of rigidified, lock-and-key type²⁸ hosts with increased affinity towards guest molecules, we here report on the molecular structures and conformations of the compounds involved in the formation of 3^I,2^{II}-anhydro-CDs, based on a molecular modeling study in conjunction with a crystallographic analysis of **3**.

2. Results and discussion

Although compounds **2** and **3** result from different regioselectivities in the course of epoxide ring opening, both are in fact stereoisomers rather than regioisomers due to the symmetry of the macrocycle. In **2**, a cis-cis type junction of a glucopyranoid ring and an altropyranose is realized via a central 1,4-dioxane ring (cf. Scheme 2). As altrose itself exhibits considerable intrinsic flexibility in which the ring adopts either a ⁴C₁ chair or an



Scheme 2. Molecular configurations and possible conformations of 3^I,2^{II}-anhydro- α -cyclodextrin: trans-diaxial epoxide ring opening (**1** \rightarrow **2**, pathway (a) in Scheme 1) conceivably results in two conformers with the altropyranose residue I adopting either the ⁴C₁ (**2a**) or ¹C₄ (**2b**) geometry. Through the alternative pathway (b) both pyranose rings retain gluco-configuration (**1** \rightarrow **3**). The central dioxane ring of each compound is highlighted by shading.

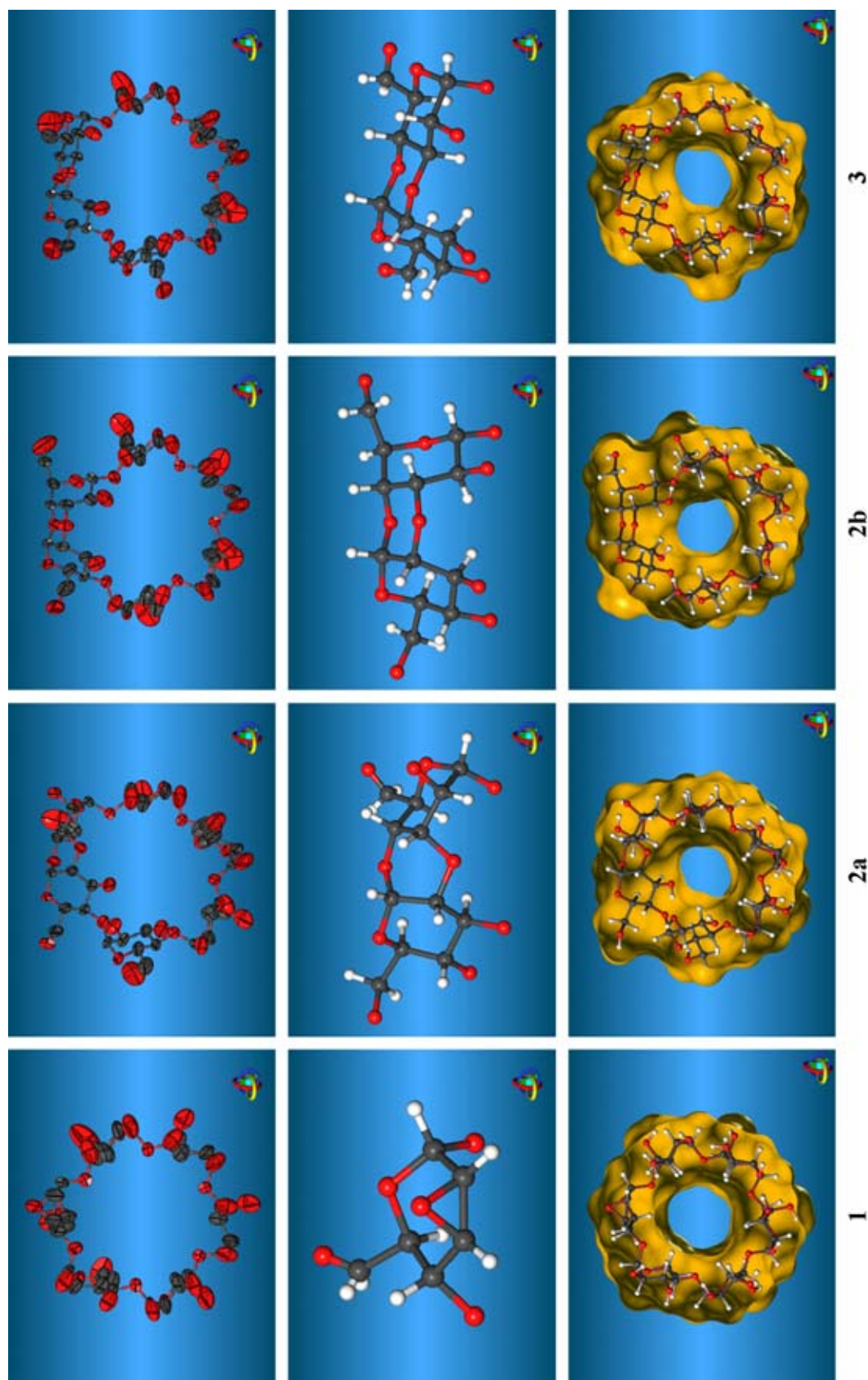


Fig. 1. Mean molecular geometries (heavy atom positions only) and anisotropic thermal ellipsoids (top row) of 2',3'-anhydro-(2'S)- α -CD (**1**) and the isomeric 3',2''-anhydro- α -CDs (**2a**, **2b**, and **3**) as derived from MD simulations in water. Center row: Enlarged ball-and-stick-type model of the sugar 2,3-epoxide unit in **1** (left) and the 3',2''-anhydro units in **2a** and **2b** (gluco/altro-configuration) as well as of **3** (gluco/glucos-steroisomer); hydroxyl-hydrogen atoms are omitted due to their flexibility. Bottom: Solvent-accessible surface models (yellow) of typical snapshot geometries extracted from the MD trajectories displaying the distorted ring conformations of the macrocycles. All molecular orientations correspond to each other, the center row models represent the topmost sugar units in the macrocycles, respectively.

Table 1

Cremer–Pople puckering parameters (Q , θ , and ϕ),^{37,38} ring conformations, and tilt angles τ ³⁹ for the pyran and dioxane rings of **1–3** (MD-derived averages with root-mean-square deviations in parentheses)

Compound	Ring	Configuration	Q (Å) ^a	θ (°) ^a	ϕ (°) ^{a,b}	Conformation	Tilt τ (°) ^c
1	I	manno	0.557(33)	50.9(5.4)	353(10.0)	^o H ₅ (\rightarrow ^o E)	100(12)
	II–VI ^d	gluco	0.620(29)	14.9(5.4)	38(24.3)	⁴ C ₁	94(12)
2a	I	altro	0.588(29)	19.2(4.9)	356(18.1)	⁴ C ₁	97.4(6.7)
	dioxane		0.759(37)	87.4(2.9)	136.3(5.5)	^{o4} , ^{c4} B	56.7(5.3)
	II	gluco	0.613(30)	14.0(5.2)	316(26.2)	⁴ C ₁	30.4(4.8)
2b	III–VI ^d	gluco	0.625(29)	15.1(5.9)	36(26.0)	⁴ C ₁	86(15)
	I	altro	0.575(33)	171.5(4.8)	190(74.0)	¹ C ₄	56.0(6.2)
	dioxane		0.547(30)	156.2(5.1)	187(16.5)	^{o3} C _{O4'} \leftrightarrow ^{c4} H _{O4}	67.7(6.0)
3	II	gluco	0.597(31)	16.2(5.8)	331(25.5)	⁴ C ₁	59.2(6.1)
	III–VI ^d	gluco	0.624(29)	16.5(5.9)	43(21.4)	⁴ C ₁	88.0(9.2)
	I	gluco	0.647(28)	6.4(3.2)	37(65.9)	⁴ C ₁	68.3(5.7)
	dioxane		0.589(29)	171.7(3.8)	242(51.4)	^{o3} C _{O4'} ^e	70.9(5.3)
	II	gluco	0.618(30)	10.8(4.6)	342(36.3)	⁴ C ₁	50.2(5.1)
	III–VI ^d	gluco	0.623(29)	15.4(5.0)	40(21.2)	⁴ C ₁	89(12)

^a Ring numbering scheme for pyranoses: O-5-C-1-C-2-C-3-C-4-C-5; dioxane rings: O-4-C-4-C-3-O-3-C-2'-C-1'.

^b For $\theta \rightarrow 0^\circ$ (⁴C₁) and $\theta \rightarrow 180^\circ$ (¹C₄), the parameter ϕ becomes insignificant.

^c Angle between the least-squares best-fit mean plane of the macrocycle (defined by all intersaccharidic O-4 atoms) and the mean plane of the pyranose or dioxane rings; values of $\tau < 90^\circ$ indicate inward tilting of the C-2 and C-3 side of the pyranoses.

^d Combined averages for all unmodified glucopyranose rings in the macrocycle.

^e ^{o3}C_{O4'} \equiv ^{o3}C_{O4} \equiv ^{c1}C_{C3}.

inverted ¹C₄ chair geometry with almost equal energies,^{20–22,25,29} two different conformers **2a** and **2b** need to be considered. In contrast, the tricyclic pyran–dioxane–pyran system in **3** features a rigid cis–trans type linkage, allowing for standard chair conformations of all six-membered rings. Similar arrangements are observed in the class of spectinomycin antibiotics and related compounds.³⁰

Molecular dynamic simulations.—A detailed conformational analysis of the structures of **2a**, **2b**, and **3** was carried out using independent molecular dynamic (MD) simulations with the explicit incorporation of water as the solvent (cf. Section 4); for comparison, their common precursor **1** was also included in this study. In each case, constant temperature ($T \approx 300$ K) and constant pressure ($P \approx 1$ bar) MD trajectories of 1 ns length were generated on periodic boxes (truncated octahedron) filled with the solute and a total of 609 TIP3-type water molecules, using CHARMM^{31,32} and a force-field adapted to properly treat carbohydrate structures.^{33,34} The MD-derived mean-solute structures, their thermal-displacement ellipsoids, as well as solvent-accessible surface^{35,36} models of typical solution snap-

shot geometries are displayed by Fig. 1. Not unexpectedly, all macrocyclic structures are characterized by rather limited flexibility of their backbones, with only the 2-OH, 3-OH, and 6-CH₂OH groups undergoing significant torsional transitions. In particular, neither MD run on conformers **2a** and **2b** displays any interconversion between these forms, both apparently being too rigid to equilibrate on the MD time scale.

Particular emphasis was put on the analysis of the pyranose and dioxane ring portions of **1–3** in terms of their geometries and their relative alignments. Table 1 gives a detailed listing of their Cremer–Pople puckering parameters^{37,38} for all six-membered rings. The combined averages over all glucopyranoses (rings II–VI in **1**, and III–VI in **2a**, **2b**, and **3**) correlate with their generally favored ⁴C₁ conformations (θ less equal approx. 16°), significant deviations are only observed for the anhydro-residues. Due to the epoxide, the ring I in **1** (Fig. 1, center row, left) adopts a typical ^oH₅ half-chair geometry (slightly distorted towards an ^oE envelope), which agrees well with previous crystallographic studies on inclusion complexes of 2,3-*per*-anhydro- α -cycloman-

nan^{6,7} and other related sugar epoxides⁴⁰ contained in the Cambridge Crystallographic Database.^{41,42}

As was already deduced from the formula drawing of Scheme 2, the cis–trans linked tricyclic system in **3** consists of rigidly anelated, almost relaxed chair-type rings even for the center dioxane portion. Significant distortions of the dioxane ring are observed for **2a** and **2b** with the ring I of the altropyranose residue adopting either the ⁴C₁ (ideal values of $\theta \approx 0^\circ$) or ¹C₄ ($\theta \approx 180^\circ$) form. In **2a**, the cis–cis-type junction forces the center ring into a strained boat form, simultaneously transferring some energy into distortions of the altrose ring I as evidenced by the rather large value of $\langle \theta \rangle = 19.2^\circ$. Most notably, a similar boat conformation was found for the center dioxane ring in the X-ray structure of cyclobis-(1 → 2)- α -D-glucopyranosyl peracetate.⁴³ For **2b**, the close spatial proximity of both axially disposed H-2^I (altrose) and H-3^{II} (glucose) protons (Fig. 1) pointing towards each other excerpts considerable strain on the center dioxane ring, which is therefore flattened (lowest puckering amplitude Q of all rings) and distorted towards a half-chair.

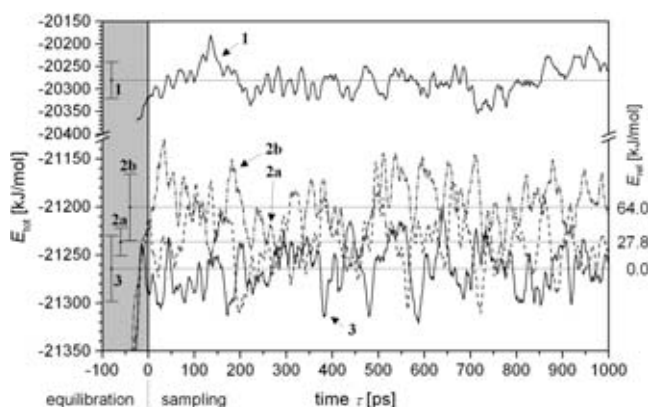


Fig. 2. Time series of total energies during the MD simulations of **1**, **2a**, **2b**, and **3** in periodic boxes (truncated octahedron) filled with 609 H₂O molecules (all box sizes approx. 33.5 ± 0.1 Å, $\langle T \rangle = 295.3$ K, $\langle P \rangle = 1$ bar), respectively, plotted as running averages smoothed over 100 configurations (5 ps) each. Negative times ($\tau = -100 - 0$ ps) indicate the equilibration phase, followed by a total data acquisition period of 1 ns. The average energies and the corresponding root-mean-square fluctuations of the energies during the sampling simulation are indicated by the dotted lines and the error bars on the left. Besides indicating the completed equilibration of all MD systems, the two conformers **2a** and **2b** appear to be 27.8 and 64.0 kJ/mol less stable than their stereoisomer **3**.

The overall molecular shape of cyclodextrins is characterized by the tilt angle τ formed between both the plane of the macrocycle and the ring plane of each sugar unit.³⁹ In general, the glucose units of unmodified CDs and their inclusion complexes are slightly tilted with their 6-CH₂OH groups pointing towards the central molecular axis, and thus the 2- and 3-OH groups form the wider opened aperture of these truncated cone-type structures.^{39,44,45} A similar trend is observed for **1** as evidenced by tilt angles larger than 90° (cf. Table 1). However, the strait-jacket of the 3^I,2^{II}-anhydro linkage in **2** and **3** leads to a considerable contraction along this torus rim: the unmodified glucose residues (rings III–VI) are aligned almost perpendicular to the macroring, whereas the rings I and II, as well as the center dioxane unit, display severe misalignments with pronouncedly decreased and inverted inclinations. The effects of very low tilt angles on the backbone structures of **1–3** become particularly evident from the solid-surface models given in Fig. 1: of all structures, both conformers **2a** and **2b** exhibit the most asymmetrically distorted over-all shapes.

The relative stabilities of the conformers **2a** and **2b** and their stereoisomer **3** are expressed in the MD-derived averages of the total energies of the simulation system, a cautious analysis made possibly by identical simulation parameters (i.e. equal temperature, pressure, box size, number of water molecules, constant set of force-field parameters, long simulation periods), despite the lack of direct conformational transitions in either unconstrained (free) or constrained (chemical or structural perturbation) form. From the plot of the total energies ($E_{\text{kin}} + E_{\text{pot}}$) of the MD systems given in Fig. 2, **3** turns out as the energetically most favorable structure, whereas **2a** and **2b** appear to be—within the limits of error—about 28 and 64 kJ/mol higher in average total energy. As deduced above, the main reasons for these relative stabilities seem to originate from strain within the cis–trans (**3**) versus cis–cis (**2a**, **2b**) type linkages in the tricyclic system and their alignments in the macrocycle.

Obviously, **3** is the thermodynamically most favored product emerging from intramolecular ring opening of the epoxide in **1**. An

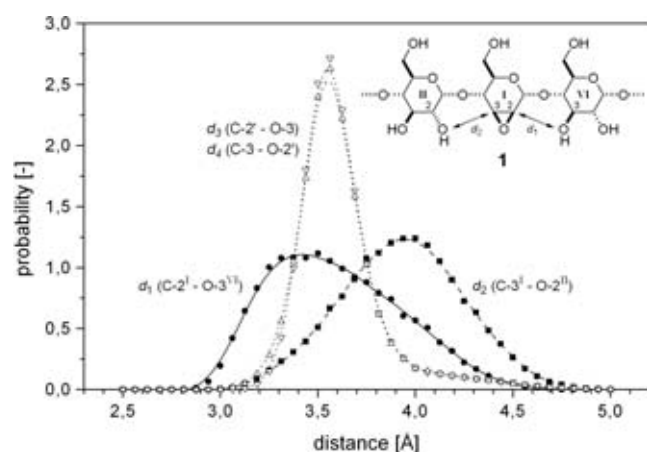


Fig. 3. Probability distributions of intramolecular distances between epoxide ring carbon atoms C-2^I and C-3^I and neighboring hydroxyl oxygen atoms O-3^{VI} and O-2^{II} as obtained from MD simulations of **1** in water. The distribution of d_1 (C-2^I...O-3^{VI}, solid line and circles) is significantly shifted towards lower distances as compared to d_2 (C-3^I...O-2^{II}, dashed line and squares), apparently favoring intramolecular attack of the 3^{VI}-OH group (**1** → **3**) over the 2^{II}-OH hydroxyl (**1** → **2**) onto the epoxide. For comparison, the distributions d_3 and d_4 of the C-2'-O-3 and C-3'-O-2' interresidue distances averaged over all neighboring unmodified glucose portions were included (triangles and dotted lines).

indication that **3** is also the kinetically preferred product of this reaction can be deduced from the comparison of intramolecular distances between the epoxide ring carbon atoms and neighboring hydroxyl oxygens suitable for attack: the probability distributions plotted in Fig. 3 display significantly shorter distances between the epoxide carbon C-2^I and O-3^{VI} ($\langle d_1 \rangle = 3.59(34)$ Å) as compared to C-3^I and O-2^{II} ($\langle d_2 \rangle = 3.93(32)$ Å), favoring the reaction **1** → **3** rather than **1** → **2**. That this effect is indeed caused by the ^oH₅ ring conformation of the 2,3-anhydro-*manno*-epoxide unit within the macrocycle is displayed by the rather equal and uniform distances C-2'...O-3 and C-3'...O-2' between all unmodified glucose units ($\langle d_3 \rangle \approx \langle d_4 \rangle \approx 3.62$ Å).

Crystallographic analysis.—Precipitation of **3** from aqueous *n*-propanol yielded crystals suitable for X-ray analysis, and thus allows comparison of its solid-state structure with the MD-derived conformation in solution. The low-temperature ($T = 173$ K) structure analysis revealed a composition of bis-(3^I,2^{II}-anhydro)- α -cyclodextrin (**3**)·3 *n*-PrOH·9 H₂O of the block-shaped, monoclinic crystals with space group $P2_1$ (cf. Fig. 4).

The CD hosts are stacked in parallel columns in an alternating head-to-head and tail-to-tail fashion. The *n*-propanol guest molecules are all located within the almost linear, nano-tube like channels formed by the columnar CD arrangement, whereas the water molecules are located without exception on interstitial positions outside of the macrocycles. As evidenced by their rather large displacement ellipsoids (Fig. 4, top left), the guest molecules retain some considerable degree of disorder even at low temperatures. As is typically observed for glucopyranose residues, all 6-CH₂OH groups on the CD hosts are twofold disordered over *gauche-gauche* (*gg*) and *gauche-trans* (*gt*) orientations, the former being favored over the latter by a ratio of 7.67:4.33 (calculated from the occupancy factors of all 12 O-6 positions included in the asymmetric unit).

The crystal architecture displays an intensive three-dimensional hydrogen bonding network, in which all hydroxyl groups and water molecules are involved; a schematic drawing is given in Fig. 5 and some distances are listed in Table 2. From the different types of hydrogen bonds observed—i.e. CD...CD intramolecular (O-3'...O-2) and intermolecular H-bonds, CD...water, water...water, CD...*n*-propanol and *n*-propanol...*n*-propanol—it is obvious that the guest molecules are not hydrogen bonded to any of the water molecules, but are shielded by their macrocyclic hosts from the water positions in the crystal environment. Of the three *n*-propanol contained in the asymmetric unit of the lattice, one is twofold H-bonded to O-2 and O-3' of the anhydro-glucopyranose portion of one molecule **3** (hydrogen bonds labeled 14 and 15 in Fig. 5 and Table 2). The remaining two *n*-propanol face each other in a head-to-head like arrangement interacting through their hydroxyl groups (H-bond no. 16); a detailed plot of this configuration is provided in Fig. 5 by the slices through the corresponding molecular surfaces. Obviously, the tube-like cavity of a dimeric unit of **3** in the crystal lattice is perfectly able to accommodate the three guest molecules *n*-PrOH with their arrangement being determined through the necessity to satisfy their hydrogen bonding requirements.

As the most characteristic feature of **3**, its ribbon model displays the significant contraction along the front aperture of the torus carrying the 2- and 3-OH groups. The unusual conicity of this CD derivative expresses itself in rather low tilt angles τ for the 3^I,2^{II}-anhydro-ring system ($\tau \approx 60^\circ$, cf. Table 3), in contrast to unmodified CDs where the 6-CH₂OH side invariably represents the narrower opening ($\tau > 100^\circ$)³⁹ of these truncated cone structures. As was already deduced for the MD derived geometry of **3**, the pyranose and diox-

ane rings adopt standard chair conformations within their rather rigid link-ups (cf. Cremer–Pople parameters^{37,38} listed in Table 3). Indeed, both independently derived structures of **3** for the crystal and solution state feature identical over-all shapes, their backbones (heavy atoms including all substituents except the O-6 atoms) being superimposable with average deviations in their atomic positions of less than 0.1 Å. Obviously, the crystal conformation of **3** undergoes no significant changes upon dissolution in water.

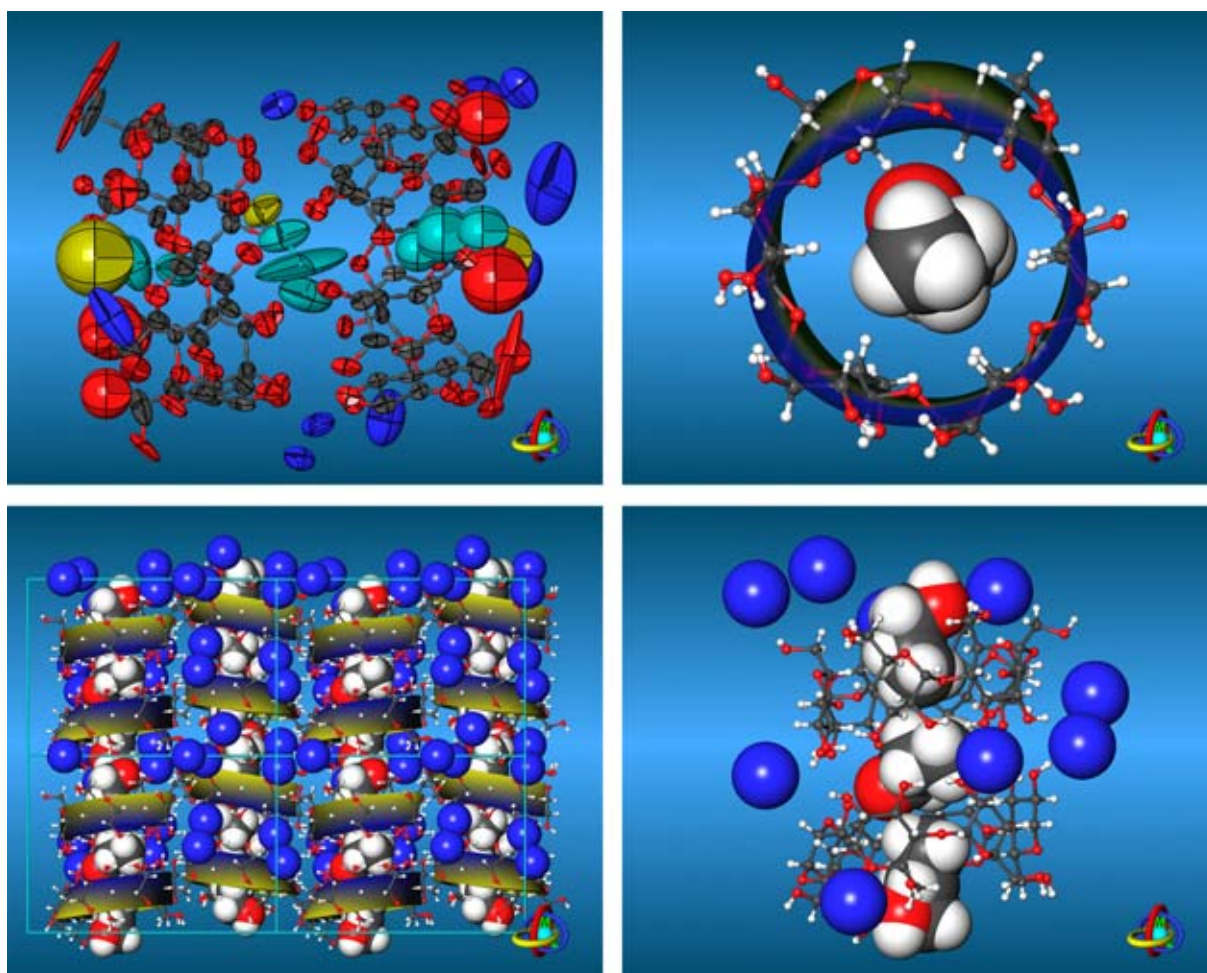


Fig. 4. Solid-state structure of 3^I,2^{II}-anhydro- α -cyclodextrin (**3**). Top left: Molecular geometry and 50% thermal ellipsoids of the asymmetric unit ($[3]_2 \cdot 3 n\text{-PrOH} \cdot 9 \text{H}_2\text{O}$); for clarity, the water oxygen atoms are colored dark blue and the *n*-propanol guests are displayed in yellow (oxygens) and cyan (carbon atoms). Top right: Single complex extracted from the asymmetric unit, the semi-transparent ribbon-model shows the distorted conicity of the host molecule (blue, ring side carrying the 2- and 3-OH groups; yellow, 6-CH₂OH) with the *n*-propanol guest (CPK model) centered along its central axis (view perpendicular to the ring plane of **3**). Bottom left: Crystal lattice (1·2·2 unit cells, view down the *a*-axis) made up of columnar head-to-head and tail-to-tail stacked anhydro-CDs (ribbon models) including almost linear and parallel assemblies of *n*-propanol guest molecules (CPK models); the guest–host arrangement being surrounded by water molecules (blue spheres) in the crystal. Bottom right: Section extracted from the lattice, displaying in detail the alignment of three guest molecules in a dimeric unit of **3**. For all ball-and-stick type models of **3** only the preferably occupied configurations of all disordered 6-CH₂OH groups were retained for the graphics.

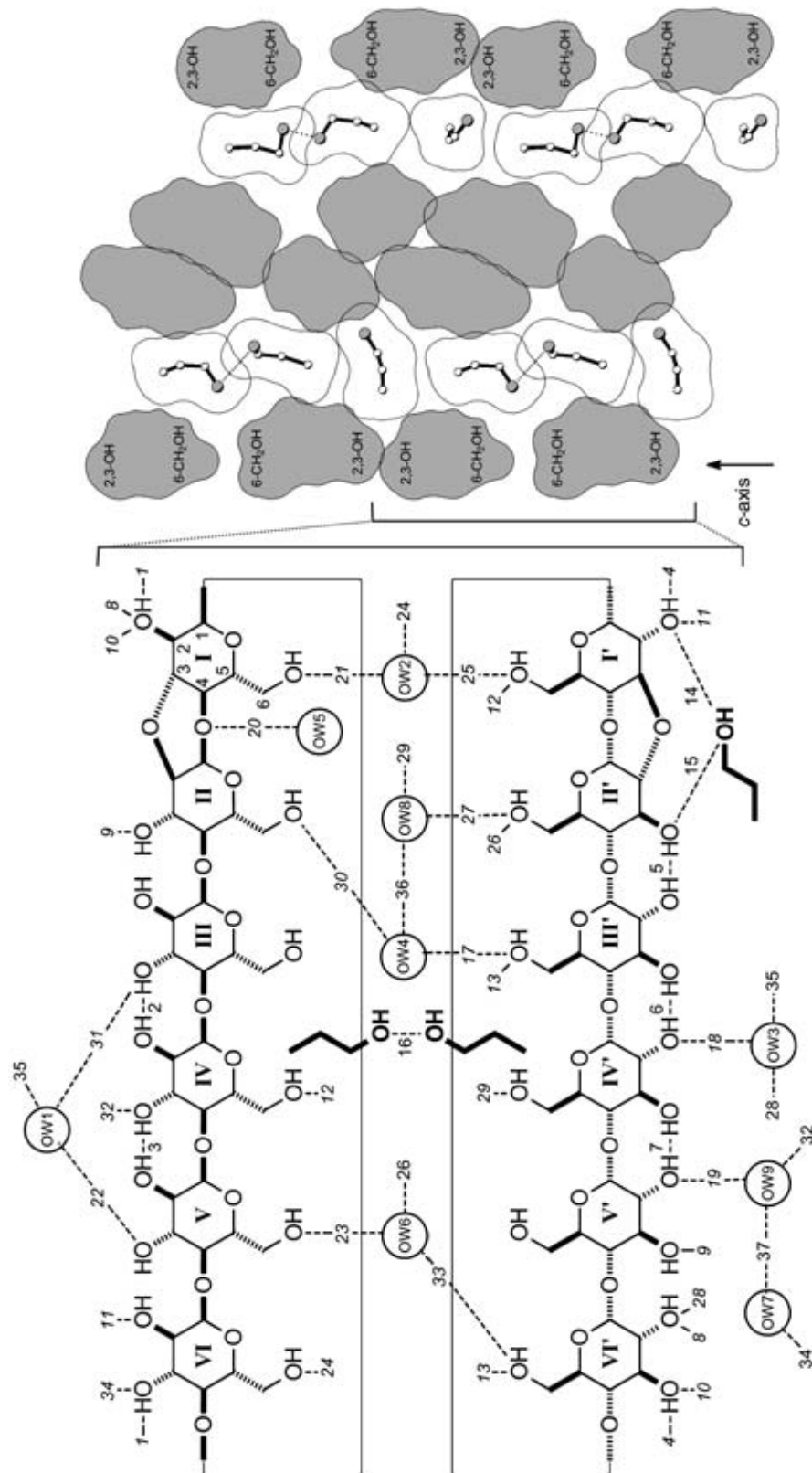


Fig. 5. Scheme of intra- and intermolecular hydrogen bonds in the solid-state structure of the bis-(3',2'1'-anhydro)- α -CD-3- η -propanol nonahydrate inclusion complex (left). The individual glucose units within the asymmetric unit are labeled I–VI and I'–VI', the water molecules OW1–OW9, the numbers in italics correspond to the indices given in Table 3. On the right, a larger segment of the crystal (four asymmetric units) displays the nano-tube like environment of stacked CD hosts into which the η -propanol guest molecules are embedded (water molecules omitted for clarity). The surface slices are given for the individual molecules, ball-and-stick type models without hydrogens are shown for η -propanol only, the CD surfaces are indicated by shading; dotted lines indicate hydrogen bonds between the guest molecules.

Table 2

Hydrogen bonds in the solid-state structure of bis-3·3 *n*-PrOH·9 H₂O, listed for acceptor...donor distances < 3.2 Å; the water molecules are labeled OW1–OW9, the glucose labeling I–VI, I'–VI', and the indices given in the first column correspond to Fig. 5

		Distance	Symmetry			Distance	Symmetry
<i>CD–CD intramolecular:</i>				<i>CD–water:</i>			
1	O(3 ^{VI})...O(2 ^I)	2.753	a	17	O(6 ^{III})...O(W4)	2.826	a
2	O(2 ^{IV})...O(3 ^{III})	2.988	a	18	O(2 ^{IV})...O(W3)	2.721	a
3	O(2 ^V)...O(3 ^{IV})	2.905	a	19	O(2 ^V)...O(W9)	2.700	a
4	O(3 ^{VI})...O(2 ^I)	2.789	a	20	O(4 ^I)...O(W5)	3.013	b
5	O(3 ^{II})...O(2 ^{III})	2.865	a	21	O(6 ^I)...O(W2)	2.626	b
6	O(3 ^{III})...O(2 ^{IV})	2.776	a	22	O(3 ^V)...O(W1)	2.847	b
7	O(3 ^{IV})...O(2 ^V)	2.815	a	23	O(6 ^V)...O(W6)	2.993	b
<i>CD–CD intermolecular:</i>				<i>water–water:</i>			
8	O(2 ^I)...O(2 ^{VI})	2.946	b	24	O(6 ^{VI})...O(W2)	2.709	b
9	O(3 ^{II})...O(3 ^V)	2.842	b	25	O(6 ^I)...O(W2)	2.222	b
10	O(2 ^I)...O(3 ^{VI})	2.855	b	26	O(6 ^{II})...O(W6)	2.903	b
11	O(2 ^I)...O(2 ^{VI})	2.858	c	27	O(6 ^{II})...O(W8)	2.811	b
12	O(6 ^I)...O(6 ^{IV})	2.619	d	28	O(2 ^{VI})...O(W3)	2.817	d
13	O(6 ^{III})...O(6 ^{VI})	2.498	e	29	O(6 ^{IV})...O(W8)	2.515	f
<i>CD–propanol:</i>				<i>water–water:</i>			
14	O(2 ^I)...O(1P)	2.787	a	30	O(6 ^{II})...O(W4)	2.926	g
15	O(3 ^{II})...O(1P)	2.766	a	31	O(3 ^{III})...O(W1)	2.879	g
<i>propanol–propanol:</i>				<i>water–water:</i>			
16	O(2P)...O(3P)	3.156	b	32	O(3 ^{IV})...O(W9)	2.827	h
				33	O(6 ^{VI})...O(W6)	2.800	l
				34	O(3 ^{VI})...O(W7)	2.816	j
				35	O(W1)...O(W3)	2.754	k
				36	O(W4)...O(W8)	2.082	b
				37	O(W7)...O(W9)	2.726	

Symmetry operations: (a) x, y, z . (b) $x, y, z-1$. (c) $x, y, z+1$. (d) $x-1, y, z$. (e) $x+1, y, z$. (f) $-x, y+1/2, -z-1$. (g) $-x, y+1/2, -z-2$. (h) $-x, y-1/2, -z-2$. (i) $-x-1, y+1/2, -z-1$. (j) $-x-1, y-1/2, -z-2$. (k) $-x, y-1/2, -z-1$.

Table 3

Selected geometry parameters (Cremer–Pople ring puckering parameters $Q/\theta/\phi$,^{37,38} and pyranose tilt angles τ ³⁹) computed for the solid-state geometry of bis-3·3 *n*-PrOH·9 H₂O; values are listed for both 3^I, 2^{II}-anhydro- α -CD molecules separately (unit 1 and 2), except for the combined averages for all eight unmodified glucose residues; see also Table 1 and the comments given there

Compound	Ring	Configuration	Q (Å)		θ (°)		ϕ (°)		Conformation	Tilt τ (°)	
			Unit 1	Unit 2	Unit 1	Unit 2	Unit 1	Unit 2		Unit 1	Unit 2
3	I	gluco	0.563	0.587	1.9	3.8	189.8	274.4	⁴ C ₁	64.8	69.0
			0.568	0.551	170.4	173.5	243.4	259.0	⁰ 3C _{O4'}	67.8	69.9
	II	gluco	0.535	0.544	16.5	12.2	297.8	294.5	⁴ C ₁	53.9	52.4
			0.557(11)		6.2(1.3)		62(18)		⁴ C ₁	97.6(6.2)	

^a Combined averages for all unmodified glucopyranose rings in both molecules of **3** with standard deviations in parentheses.

3. Conclusions

Although intramolecular opening of epoxide **1** by the 3-OH of a neighboring glucose unit occurs in an unexpected diequatorial fashion to afford **3** in high yield, MD calculations reveal **3** to be the favored product when comparing the average total energies of the

stereoisomers **2a**, **2b**, and **3** in simulated water boxes. Provided that atomic distances are a decisive factor for the regioselectivity of epoxide opening, **3** also turns out to be the kinetically preferred product. The over-all molecular shape of this rigid CD derivative, as evident from its solid-state structure, not only undergoes little changes upon dissolution in

water retaining its unusual conicity caused by the contracted tricyclic pyran–dioxane–pyran ring system, but also provides a picture of an inclusion complex of **3** with *n*-propanol.

4. Experimental

Molecular dynamics simulations.—The starting geometries of **1**, **2a**, **2b**, and **3** were generated by editing the solid-state geometry of α -CD⁴⁶ and subsequent single-point energy minimization. All MD simulations starting from these structures were carried out using CHARMM^{31,32} with a force-field particularly adapted for the treatment of carbohydrates^{33,34} and explicit incorporation of water as the solvent. Each compound was centered in a periodic box (truncated octahedron) filled with pre-equilibrated TIP3-type water, yielding—after removal of the solvent molecules that overlap with the solute—simulation systems including 609 water molecules, respectively. After full-lattice energy minimizations, all boxes were slowly heated from 0 to 300 K within a 15 ps MD time frame, and subsequently equilibrated for an additional 85 ps; the final MD data were sampled using simulations of 1 ns in each case, molecular configurations were saved every 50 fs for analysis purposes. All MD runs were carried for constant pressure ($P_{\text{ref}} = 1$ atm, isothermal compressibility 4.63×10^{-5} atm⁻¹, pressure coupling constant $\tau_p = 5$ ps) and constant temperature ($T_{\text{ref}} = 300$ K, temperature coupling constant $\tau_T = 5$ ps, allowed temperature deviation $\Delta T = \pm 10$ K) conditions (*NPT* ensemble) using the following simulation

parameters: timestep $\Delta t = 1$ fs (leap-frog integrator, all X–H bond lengths were constrained using the SHAKE protocol⁴⁷), dielectric constant $\epsilon = 1.0$, cut-off distance for long-range interactions 12 Å, cut-off radius for images in atom lists 13 Å; for some specific parameters recalculated from the MD trajectories see Table 4.

For each MD time series, the mean solute geometry was obtained by 3D fitting of all configurations (heavy atoms only, excluding CH₂OH-oxygen atoms); the best-fit models from this procedure were selected as representative molecular geometries in aqueous solution (Fig. 1, center and bottom row). The corresponding atomic anisotropic thermal displacement ellipsoids (cf. Fig. 1, top row) were obtained from diagonalization of the displacement tensor calculated from all atomic displacement vectors (for each atom, the eigenvectors and the root of the eigenvalues of this tensor yield the principal axis of the thermal ellipsoid and the root-mean-square atomic displacements along these directions).⁴⁸

Crystal structure of bis-(3^I,2^{II}-anhydro)- α -cyclodextrin·3 *n*-PrOH·9 H₂O.—A mixture of 60 mg of **3**, 100 μ L of water and 100 μ L of *n*-propanol was heated up to 90 °C to give a clear solution and then filtered through a membrane filter PTFE (pore size, 0.5 μ m; TOSOH). The filtrate was sealed and allowed to stand at rt for 1 week to yield colorless, block-shaped crystals with parameters as follows: $M_r = 1126.04$ g/mol, monoclinic, space group $P2_1$, $a = 14.257(1)$, $b = 22.623(2)$, $c = 16.644(1)$ Å, $\beta = 104.82(1)^\circ$, $V = 5189.7(7)$ Å³, $Z = 4$, $\rho = 1.414$ g/cm, $\mu(\text{Mo K}\alpha) = 0.126$

Table 4

Selected MD simulation parameters recalculated from the time series (all MD systems include 609 H₂O molecules, $M_{\text{tot}} = 11926.42$ g/mol) with standard deviations in parentheses

Compound	T [K]	E_{tot} (kJ/mol)	E_{kin} (kJ/mol)	E_{pot} (kJ/mol)	E_{rel} (kJ/mol) ^a	Box size (Å)	Volume (Å ³) ^b	Density σ (g/cm ³)
1	295.2(5.3)	−20,281(41)	4863(88)	−25,143(98)		33.47(6)	18,740(135)	1.057(8)
2a	295.3(5.3)	−21,237(14)	4864(88)	−26,101(107)	27.9	33.46(9)	18,726(142)	1.057(8)
2b	295.2(5.3)	−21,200(35)	4863(88)	−26,063(100)	64.0	33.47(6)	18,747(141)	1.056(8)
3	295.3(5.3)	−21,264(34)	4864(87)	−26,129(96)	0.0	33.47(9)	18,747(129)	1.056(7)

^a Relative total energies for the 3^I,2^{II}-anhydro- α -cyclodextrins **2a**, **2b**, and **3** only.

^b Volume = (box size)³/2.0 for the truncated octahedron.

mm⁻¹, crystal dimensions 0.5 × 0.4 × 0.15 mm, $T = 173(2)$ K. Of 29,184 reflections collected on a Siemens CCD three-circle diffractometer using graphite-monochromated Mo K_α ($\lambda = 0.71073$ Å) radiation, 19,278 are independent ($R_{\text{int}} = 0.0585$); θ range of data collection 1.27–28.01°, completeness to $\theta = 28.01^\circ$ 82.4%, limiting indices h : $-16 \rightarrow 15$, k : $-28 \rightarrow 29$, and l : $-16 \rightarrow 21$. The structure was solved by shake and bake methods⁴⁹ and successive Fourier synthesis. Refinement (on F^2) was performed by full-matrix least-squares method (19,278 reflections, 18 restraints, 1403 independent parameters).⁵⁰ $R(F) = 0.1017$ for reflections with $I > 2\sigma(I)$, $wR(F^2) = 0.2193$ for 19,278 reflections ($w = 1/[\sigma^2(F_o^2) + (0.1337P)^2 + 4.1868P]$); where $P = (F_o^2 + 2F_c^2)/3$; $R(F) = 0.2205$ and $wR(F^2) = 0.2966$ for all reflections. The final goodness-of-fit on F^2 equals 1.005, the largest difference peak and hole of electron density are +0.503 and -0.296 e Å³, respectively. All bond length and angles fall within normal ranges for carbohydrate structures.

All 6-CH₂OH groups on both cyclodextrin units are twofold disordered over the gauche–gauche (gg , torsion angle ω O₅–C₅–C₆–O₆ approx. -60°) and the gauche–trans (gt , $\omega \approx +60^\circ$) orientation, with the former being favored over the latter by a ratio of 7.67:4.33 based on relative occupancy factors. All non-hydrogen atoms (except of one n -propanol molecule and eight of the 12 O-6 position with lower occupancy) were refined anisotropically, hydrogen atoms were positioned geometrically and considered in calculated positions with the $1.2U_{\text{eq}}$ value of the corresponding bound atom. The ribbon models of **3** (Fig. 4) were computed by connecting the centers and normal vectors of the least-squares best-fit mean planes of all pyranose rings (without substituents) via cubic splines.⁴⁸

5. Supplementary material

Crystallographic data (excluding structure factors) for the structure in this paper have been deposited with the Cambridge Crystallographic Data Centre as supplementary publication no. CCDC-168467. Copies of the data

can be obtained, free of charge, on application to The Director, CCDC, 12 Union Road, Cambridge CB2 1EZ, UK, (fax: +44-1223-336033 or e-mail: deposit@ccdc.cam.ac.uk or www: <http://www.ccdc.cam.ac.uk>).

Acknowledgements

The authors are grateful to Professor F.W. Lichtenthaler (S.I.) for prolific discussions and carefully editing the manuscript, and Professor H.J. Lindner (M.B.) for lucid suggestions.

References

1. Immel, S.; Lichtenthaler, F. W.; Lindner, H. J.; Nakagawa, T. *Tetrahedron: Asymmetry* **2001**, *12*, in press.
2. Fujita, K.; Nagamura, S.; Imoto, T. *Tetrahedron Lett.* **1984**, *25*, 5673–5676.
3. Ikeda, H.; Nagano, Y.; Du, Y.; Ikeda, T.; Toda, F. *Tetrahedron Lett.* **1990**, *31*, 5045–5048.
4. Coleman, A. W.; Zhang, P.; Ling, C. C.; Mahuteau, J.; Parrot-Lopez, H.; Miocque, M. *Supramol. Chem.* **1992**, *1*, 11–14.
5. Zhang, P.; Coleman, A. W. *Supramol. Chem.* **1993**, *2*, 255–263.
6. Immel, S.; Fujita, K.; Lindner, H. J.; Nogami, Y.; Lichtenthaler, F. W. *Chem. Eur. J.* **2000**, *6*, 2327–2333.
7. Immel, S.; Lichtenthaler, F. W.; Lindner, H. J.; Fujita, K.; Fukudome, M.; Nogami, Y. *Tetrahedron: Asymmetry* **2000**, *11*, 27–36.
8. Khan, A. R.; Barton, L.; D'Souza, V. T. *J. Chem. Soc., Chem. Commun.* **1992**, 1112–1114.
9. Khan, A. R.; Barton, L.; D'Souza, V. T. *J. Org. Chem.* **1996**, *61*, 8301–8303.
10. Isac-Garcia, J.; Lopez-Paz, M.; Santoyo-Gonzalez, F. *Carbohydr. Lett.* **1998**, *3*, 109–116.
11. Khan, A. R.; Forgo, P.; Stine, K. J.; D'Souza, V. T. *Chem. Rev.* **1998**, *98*, 1977–1996.
12. Gattuso, G.; Nepogodiev, S. A.; Stoddart, J. F. *Chem. Rev.* **1998**, *98*, 1919–1958.
13. Kelly, D. R.; Mish'al, A. K. *Tetrahedron: Asymmetry* **1999**, *10*, 3627–3648.
14. Fujita, K.; Ohta, K.; Ikegami, Y.; Shimada, H.; Tahara, T.; Nogami, Y.; Koga, T.; Saito, K.; Nakajima, T. *Tetrahedron Lett.* **1994**, *35*, 9577–9580.
15. Harata, K.; Nagano, Y.; Ikeda, H.; Ikeda, T.; Ueno, A.; Toda, F. *J. Chem. Soc., Chem. Commun.* **1996**, 2347–2348.
16. Fujita, K.; Chen, W.-H.; Yuan, D.-Q.; Nogami, Y.; Koga, T.; Fujioka, T.; Mihashi, K.; Immel, S.; Lichtenthaler, F. W. *Tetrahedron: Asymmetry* **1999**, *10*, 1689–1696.
17. Ohta, K.; Fujita, K.; Shimada, H.; Ikegami, Y.; Nogami, Y.; Koga, T. *Chem. Pharm. Bull.* **1997**, *45*, 631–635.
18. Fujita, K.; Shimada, H.; Ohta, K.; Nogami, Y.; Nasu, K.; Koga, T. *Angew. Chem., Int. Ed. Engl.* **1995**, *34*, 1621–1622.
19. Nogami, Y.; Fujita, K.; Ohta, K.; Nasu, K.; Shimada, H.; Shinohara, C.; Koga, T. *J. Inclusion Phenom. Mol. Recognit. Chem.* **1996**, *25*, 57–60.

20. Nogami, Y.; Nasu, K.; Koga, T.; Ohta, K.; Fujita, K.; Immel, S.; Lindner, H. J.; Schmitt, G. E.; Lichtenthaler, F. W. *Angew. Chem., Int. Ed. Engl.* **1997**, *36*, 1899–1902.
21. Fujita, K.; Ohta, K.; Nogami, Y.; Nasu, K.; Shiratani, T.; Sudo, M.; Koga, T. In *Proceedings of the 9th International Symposium on Cyclodextrins, Santiago de Compostela, Spain, May 31–June 3*; Torres Labandeira, J. J.; Vila-Jato, J. L., Eds.; Kluwer Academic: Dordrecht/Boston, 1999; pp. 113–115.
22. Immel, S.; Fujita, K.; Lichtenthaler, F. W. *Chem. Eur. J.* **1999**, *5*, 3185–3192.
23. Yan, J.; Watanabe, R.; Yamaguchi, M.; Yuan, D.-Q.; Fujita, K. *Tetrahedron Lett.* **1999**, *40*, 1513–1514.
24. Fujita, K.; Tahara, T.; Sasaki, H.; Egashira, Y.; Shingu, T.; Imoto, T.; Koga, T. *Chem. Lett.* **1989**, 917–920.
25. Immel, S. In *Proceedings of the 10th International Symposium on Cyclodextrins, May 21–24*; Szejtli, J., Ed.; MIA Digital Publishers: Ann Arbor, MI, 2000; pp. 274–281.
26. Koshland, Jr., D. E. *Angew. Chem., Int. Ed. Engl.* **1994**, *33*, 2475–2478.
27. Fujita, K.; Okabe, Y.; Ohta, K.; Yamamura, H.; Tahara, T.; Nogami, Y.; Koga, T. *Tetrahedron Lett.* **1996**, *37*, 1825–1828.
28. Lichtenthaler, F. W. *Angew. Chem., Int. Ed. Engl.* **1994**, *33*, 2364–2374.
29. Lichtenthaler, F. W.; Mondel, S. *Carbohydr. Res.* **1997**, *303*, 293–302.
30. Cuny, E.; Lichtenthaler, W.; Lindner, H. J. *Acta Crystallogr., Sect. C* **1994**, *50*, 1599–1601.
31. Brooks, B. R.; Bruccoleri, R. E.; Olafson, B. D.; States, D. J.; Swaminathan, S.; Karplus, M. *J. Comput. Chem.* **1983**, *4*, 187–217.
32. Nilsson, L.; Karplus, M. *J. Comput. Chem.* **1986**, *7*, 591–616.
33. Reiling, S.; Schlenkrich, M.; Brickmann, J. *J. Comput. Chem.* **1996**, *17*, 450–468.
34. Reiling, S.; Brickmann, J. *Macromol. Theory Simul.* **1995**, *4*, 725–743.
35. Connolly, M. L. *J. Appl. Crystallogr.* **1983**, *16*, 548–558.
36. Connolly, M. L. *Science* **1983**, *221*, 709–713.
37. Cremer, D.; Pople, J. A. *J. Am. Chem. Soc.* **1975**, *97*, 1354–1358.
38. Jeffrey, G. A.; Yates, J. H. *Carbohydr. Res.* **1979**, *74*, 319–322.
39. Lichtenthaler, F. W.; Immel, S. *Liebigs Ann.* **1996**, 27–37.
40. Wu, X.; Kong, F.; Lu, D.; Li, G. *Carbohydr. Res.* **1992**, *235*, 163–178.
41. Allen, F. H.; Ballard, S.; Brice, M. D.; Cartwright, B. A.; Doubleday, A.; Higgs, H.; Hummelink, T.; Hummelink-Peters, B. G.; Kennard, O.; Motherwell, W. D. S.; Rodgers, J. R.; Watson, D. G. *Acta Crystallogr., Sect. B* **1979**, *35*, 2331–2339.
42. Allen, F. H.; Kennard, O.; Taylor, R. *Acc. Chem. Res.* **1983**, *16*, 146–153.
43. Pozsgay, V.; Dubois, E. P.; Lotter, H.; Neszmelyi, A. *Carbohydr. Res.* **1997**, *303*, 165–173.
44. Lipkowitz, K. B.; Green, K.; Yang, J. A. *Chirality* **1992**, *4*, 205–215.
45. Saenger, W.; Jacob, J.; Gessler, K.; Steiner, T.; Hoffmann, D.; Sanbe, H.; Koizumi, K.; Smith, S. M.; Takaha, T. *Chem. Rev.* **1998**, *98*, 1787–1802.
46. Chacko, K. K.; Saenger, W. *J. Am. Chem. Soc.* **1981**, *103*, 1708–1715.
47. Van Gunsteren, W. F.; Berendsen, H. J. C. *Mol. Phys.* **1977**, *34*, 1311–1327.
48. Immel, S. *MOLARCH⁺: Molecular Architecture Modeling Program V6.15*; Technical University of Darmstadt: Germany, 2001.
49. Sheldrick, G. M. *SHELXD-97: Program for Crystal Structure Solution of Macromolecules*; University of Göttingen: Germany, 2000.
50. Sheldrick, G. M. *SHELXL-97: Program for Crystal Structure Refinement*; University of Göttingen: Germany, 1997.

The First Successful Crystallographic Characterization of a Cyclodextrin Dimer: Efficient Synthesis and Molecular Geometry of a Doubly Sulfur-Bridged β -Cyclodextrin**

De-Qi Yuan,^[b] Stefan Immel,^{*[a]} Katzutaka Koga,^[b] Masatoshi Yamaguchi,^[c] and Kahee Fujita^[b]

Abstract: β -Cyclodextrin is transannularly disulfonylated at the 6^A- and 6^B-positions, and then converted to the corresponding 6^A,6^B-diiodide and 6^A,6^B-dithiol. Cross-coupling of the latter two species yields a single head-to-head-coupled β -cyclodextrin dimer **5** with two sulfur linkers at adjacent 6-methylene carbons. NMR and X-ray analysis

revealed the *trans*-type (“aversive”) linkage of both β -cyclodextrin units. In the solid-state structure of **5**·5MeOH·23H₂O, the undistorted cyclodextrin

macrocycles feature almost parallel ring planes pointing away from each other, leaving **5** with a “handcuff-like” appearance of approximate C₂ symmetry. This work represents the first successful crystallographic study on a cyclodextrin dimer.

Keywords: cross-coupling · cyclodextrins · molecular structure · sulfide-bridges · X-ray diffraction

Introduction

Exciting achievements have been witnessed with cyclodextrins (CDs) as artificial hosts in many of the most actively pursued research fields, such as drug delivery systems, molecular sensing technologies, biomimetic recognition, and catalysis.^[1] However, the recognition ability of native CDs is greatly confined by their C_n symmetry and limitations in cavity size, shape, flexibility, and hydrophobicity. Bridging two or more CD units together provides a promising way to alter both the binding ability and guest selectivity. In the pioneering works, Tabushi synthesized a doubly bridged β -CD dimer with two ethylenediamine spacers,^[2] and Fujita found that the two CD moieties of disulfide-bridged β -CD could cooperate in the binding of ethyl orange, yielding an association constant about

220 times that of β -CD.^[3] Breslow et al. demonstrated that the same CD dimer selectively bound appropriate “ditopic guests” almost as strongly as antigen–antibody binding.^[4] Large varieties of CD dimers have been synthesized in which two CD units are linked on either their primary or secondary face by single or double linkers ranging from single atoms to oligopeptide segments.^[5] Heterodimers,^[6] -trimers,^[7] and -tetramers^[8] have also been reported. The *cis* forms of doubly bridged CD dimers were found to bind appropriate guests with very high affinities and shape selectivities.^[9] Nolte et al. demonstrated that, depending on the nature of linkers, CD dimers can bind tetrakis(sulfophenyl)porphyrin to form 1:1 *syn*-, *syn/anti*-, and 2:2 (crossed double-zigzag-type) complexes.^[10] CD dimers were found to have sequence-selective binding ability toward peptides and to disrupt protein aggregation.^[11] Catalytic functionalities within the linker or on the rims of a dimer may result in strong catalysis. For example, the La^{III} complex of a bipyridyl-bridged β -CD dimer has been used to significantly enhance the hydrolysis of phosphodiesteres,^[12] thiazolio-appended CD dimers were used to promote benzoin condensation,^[13] Se–Se-bridged CD dimers were used to effect glutathione peroxidase-like activity,^[14] CD-sandwiched metalloporphyrin has been used to catalyze the epoxidation of alkene,^[15] metalloporphyrin-based CD tetramers have been used to demonstrate site-specific oxidation of steroids,^[16] and β -carotene^[17] and, quite recently, EDTA–Ce^{IV}-bridged CD dimers have been used to amplify luminol chemiluminescence,^[18] among many others.

Undoubtedly, three-dimensional structural information on the CD oligomers is very important for understanding the

[a] Dr. S. Immel
Clemens Schöpf-Institut für Organische Chemie und Biochemie
Technische Universität Darmstadt
Petersenstrasse 22, 64287 Darmstadt (Germany)
Fax: (+49) 6151-166674
E-mail: lemmit@sugar.oc.chemie.tu-darmstadt.de

[b] Prof. Dr. De-Q. Yuan, Prof. Dr. K. Koga, Prof. Dr. K. Fujita
Faculty of Pharmaceutical Sciences, Nagasaki University
Bunkyo-machi, Nagasaki 852-8521 (Japan)

[c] Dr. M. Yamaguchi
Faculty of Pharmaceutical Sciences, Fukuoka University
Nanakuma, Jonan-ku, Fukuoka 814-0180 (Japan)

[**] Molecular Modeling of Saccharides, Part 31; for Part 30 see: S. Immel, K. Fujita, M. Fukudome, M. Bolte, *Carbohydr. Res.* **2001**, *336*, 297–308.

FULL PAPER

S. Immel et al.

process of molecular recognition by CD dimers.^[19] Unfortunately, we know surprisingly little about the spatial structures of CD oligomers in spite of the many efforts directed to their synthesis and properties. We do not even have enough knowledge to make a convincing judgment on the most fundamental aspects of the large host molecules: do the two or more CD cavities distort or not upon being bridged? How are they spatially arranged? In the following we report a highly efficient synthesis of a new β -CD dimer with two very short sulfur linkers and its unequivocal structural characterization through NMR analysis. Single-crystal X-ray-diffraction analysis was employed for the first time to obtain structural information on a CD dimer and it successfully afforded a clear image of the solid-state structure of the doubly sulfur-bridged β -CD dimer.

Results and Discussion

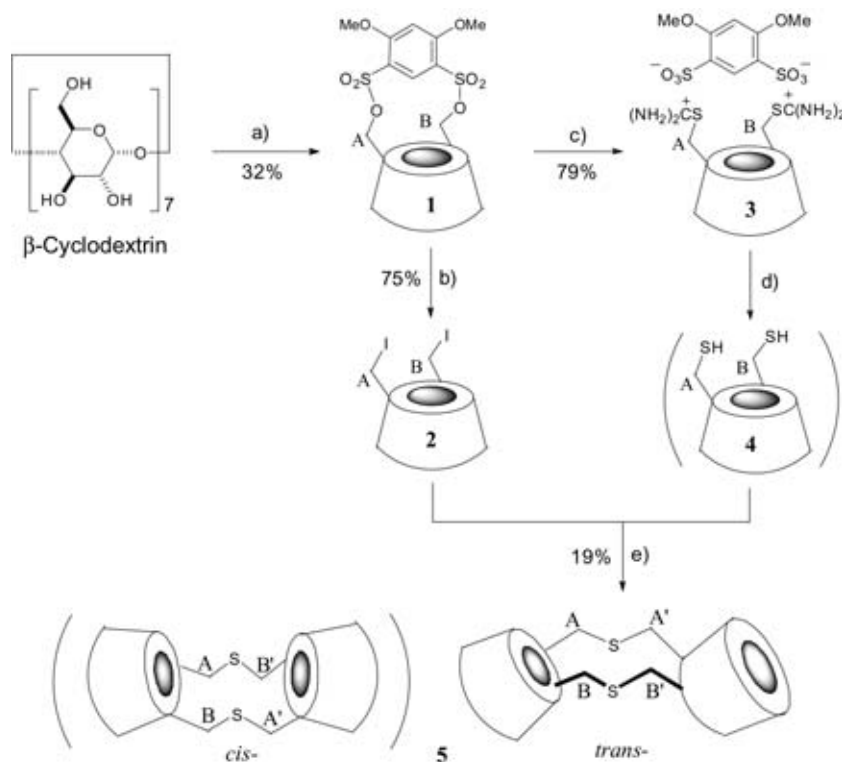
The synthetic approach to the doubly bridged CD dimer is depicted in Scheme 1. β -CD was selectively activated by employing the “looper’s walk” method.^[20] Treatment of β -CD with 4,6-dimethoxy-1,3-benzenedisulfonyl chloride in dry pyridine afforded the 6^A,6^B-capped CD **1**,^[21] whose yield is clearly dependent on the molar ratio of capping reagent to CD. Utilization of the capping reagent in 50% excess ensured a good yield of the capped product **1**, usually ranging from 30 to 40%. Compound **1** was converted to the corresponding 6^A,6^B-diiodide **2** by stirring a mixture of **1** and KI in DMF at 80 °C. Treatment of **1** with thiourea in DMF gave the

thiuronium salt **3** in 79% yield. This was treated with 0.25 N aqueous NaOH, and the generated 6^A,6^B-dithiol **4** was collected by precipitation with acetone. The crude 6^A,6^B-dithiol **4** was used in the following reaction without further purification. Reaction of the dithiol **4** and diiodide **2** was carried out in DMF in the presence of Cs₂CO₃ at room temperature and under an argon atmosphere. Reversed-phase chromatography of the reaction mixture afforded the doubly bridged β -CD dimer **5** in 19% yield. The FAB-MS spectrum showed the molecular peak [*M*⁺] at *m/z* = 2266.1, consistent with the expected structure of a doubly bridged β -CD dimer with two sulfur linkers (calcd C₈₄H₁₃₆O₆₆S₂⁺: 2266.2).

In principal, two isomeric head-to-head β -CD dimers may be formed in the course of the cross-coupling reaction, with either a *cis*-type linkage across the glucose 6^A,6^B- and 6^B,6^A-positions, or alternatively a *trans* connection of the 6^A,6^A and 6^B,6^B type. Both isomers retain C₂ symmetry, yet differ substantially in their molecular shapes: the *cis* isomer is expected to adopt a compact, occlusive geometry (“clamshell”),^[9] whereas the *trans* compound should be characterized by an extended, aversive appearance (“loveseat”).^[9] However, NMR spectra of the isolated product indicate the presence of only a single isomer, the alternative form was not recognized from the fractions of column chromatography.

Both the ¹H and ¹³C NMR spectra of **5** (Figure 1) maintain the basic pattern of β -CD, the weaker signals shifted out from the normal ones are related to the modified sugar residues. Partial assignment of the spectra based on 2D COSY experiment reveals only two sorts of functional glucosides; this confirms the C₂ symmetry of the dimer. Both of them demonstrated significant upfield shifts for their methylene geminal protons (up to the range of 2.75–3.25 ppm), a moderate upfield shift for H-4 and small to moderate downfield shifts for H-5, but trivial shifts for H-1, H-2 and H-3. The ¹³C NMR spectrum demonstrated remarkable upfield shifts for C-6, small upfield shifts for C-5, and downfield shifts for C-4 of the modified sugar units. This chemical shift pattern is in good agreement with the replacement of the primary hydroxyl groups by alkyl thiols. Apart from the modified units, no other glucosides showed meaningful shifts. These observations suggest that no apparent distortion should have occurred in the hydrophobic cavities of the doubly bridged CD dimer.

The assignment of the bridging mode (*cis*- or *trans*- with respect to the ring containing both linkers) of the dimer is attempted by using NMR tech-



Scheme 1. Synthesis of the doubly bridged β -CD dimer **5**. a) 1.5 equiv 4,6-dimethoxy-1,3-benzenedisulfonyl chloride, dry pyridine, 40 °C, 2.5 h. b) KI, DMF, 80 °C, 4.5 h. c) Thiourea, DMF, 90 °C, 20 h. d) 0.25 N aqueous NaOH, 90 °C, 10 min; NaBH₄, RT, 10 min. e) Cs₂CO₃, DMF, Ar gas, RT, 66 h.

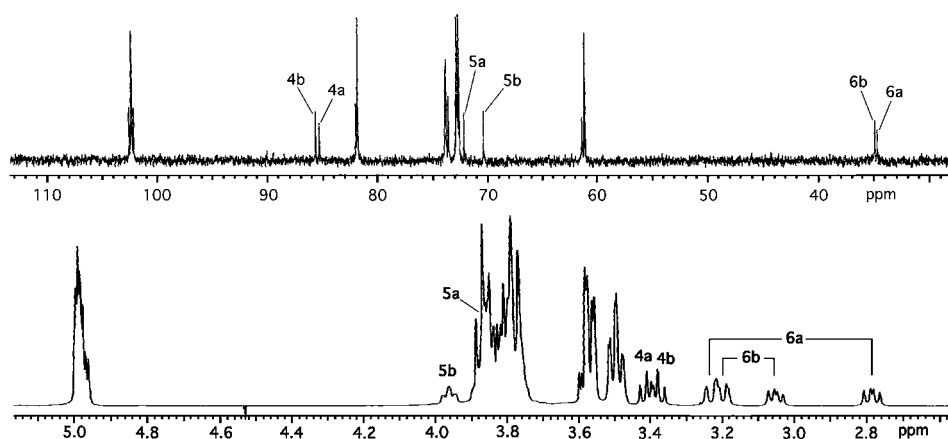


Figure 1. ^1H and ^{13}C NMR spectra of β -CD dimer **5** (D_2O , CH_3CN int.).

niques. In the *cis* structure, each sulfur atom bridges the “A” glucoside of one CD moiety and “B” glucoside of another, that is, the two sorts of modified sugar residues are correlated by one sulfur atom. This correlation is expected to be probed by the HMBC (heteronuclear multiple bond correlation) method.^[22] In the *trans* isomer, each sulfur connects one pair of equivalent sugar residues, thus no HMBC signals are expected to appear between the two sorts of modified sugar residues. As shown in Figure 2, no cross-signals were observed between the two sorts of modified methylene groups; this suggests a *trans* structure for dimer **5**. This assignment is confirmed by the result of single-crystal X-ray diffraction.

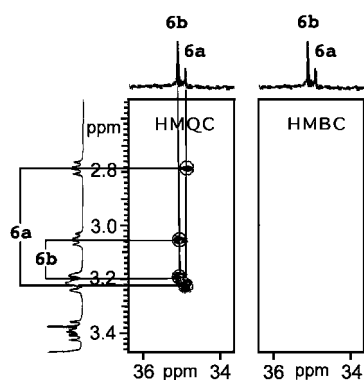


Figure 2. HMQC and HMBC spectra of **5** (only the modified methylene part is shown for clarity). No HMBC cross signals appeared between 6a and 6b; this suggests a *trans*-structure for **5**.

Solid-state structure analysis of 5: Single crystals of **5** were obtained after chromatographic purification as described above. Low-temperature X-ray analysis revealed a crystal composition of $\mathbf{5} \cdot 5\text{MeOH} \cdot 23\text{H}_2\text{O}$, the molecular and crystal structures are displayed in Figure 3, unequivocally establishing the *trans*-type linkage of the β -CD moieties and the approximate C_2 symmetry of **5**. The β -CD dimers are packed in a herringbone-like fashion forming individual cavities that are blocked by adjacent CD rings and thus do not form tube-like channels. The β -CD cavities are partially filled with four and five water molecules of crystallization, the other water molecules and methanol fill interstitial positions between

the macrocycles. All hydroxyl groups and oxygen atoms participate in the formation of a three-dimensional hydrogen-bonding network in the crystal lattice.

For the dimeric β -CD unit a few relevant geometry descriptors are listed in Table 1, a comprehensive list of atomic coordinates and all bond length and angles—all of which are within standard ranges for organic compounds—may be obtained from the data deposited with the Cambridge Crystallographic Data Centre (see Experimental Section). The molecular geometry of **5** is characterized by an almost coplanar alignment of the $\text{C6}^{\text{A}}\text{-S-C6}^{\text{A}}$ and $\text{C6}^{\text{B}}\text{-S-C6}^{\text{B}}$ fragments within the sulfur linkages, with the shape of an elongated planar hexagon. Within this linkage, the O6-C5-C6-S dihedral angles invariably adopt (*-*)-*gauche* arrangements, yet the calculated values for the $\text{C5-C6-S-C6}'$ torsion angles differ significantly at both positions (approx. 75° and -130° , cf. Table 1).

Table 1. Selected geometry parameters for the dimeric β -CD unit as calculated from the solid-structure of $\mathbf{5} \cdot 5\text{MeOH} \cdot 23\text{H}_2\text{O}$.

Linkage	A – A'	B – B'	
torsion angles [°]			
O5-C5-C6-S	–45.7	–68.9	
C5-C6-S-C6'	–128.1	75.5	
C6-S-C6'-C5'	–133.6	76.1	
S-C6'-C5'-O5'	–44.5	–67.2	
CD unit	I	II	
tilt angle ^[a]	τ [°]	103 ± 8	104 ± 9
ring diameter ^[b]	r [Å]	9.86 ± 0.26	9.85 ± 0.47
ring puckering ^[c]	d [Å]	0.12 ± 0.06	0.06 ± 0.03
inclination ^[d]	[°]	2.9	2.9

[a] Angle between the least-squares best-fit mean plane of the macrocycle (defined by all intersaccharidic O4 atoms) and the mean plane of the pyranose rings (atoms O5 and C1–C5); values of $\tau > 90^\circ$ indicate outward tilting of the C2 and C3 side of the glucoses; parameter averaged over all glucose residues. [b] Average $\text{O4-O4}''$ separations within the CD macrocycles. [c] Average deviation of all O4-atoms of the CD macrocycles from planarity. [d] Angle between the least-squares best-fit mean ring planes (all O4 atoms) of both linked β -CD units.

Both linked β -CD-rings feature almost parallel mean ring planes with a relative inclination of only 2.9° ; the centers of the two cavities being 13.6 \AA apart. The geometries of the β -CD units are within the usual ranges observed for these compounds and their complexes^[24, 25] (tilt angles τ ^[25] of the glucose residues in relation to the macroring of approx. 105° , ring diameters of about 9.9 \AA). As evidenced by their Cremer–Pople parameters^[26] Q , θ , and ϕ , all glucose units adopt standard $^4\text{C}_1$ chair conformations ($Q \approx 0.563 \pm 0.018 \text{ \AA}$, $\theta \approx 4 \pm 2^\circ$, ϕ is not significant). Out of the total of ten $6\text{-CH}_2\text{OH}$ groups six adopt *gauche-trans* (*gt*) arrangements with O5-C5-C6-O6 -torsion angles of $\omega \approx +60^\circ$, the remaining four are in *gauche-gauche* (*gg*) orientations ($\omega \approx -60^\circ$) and

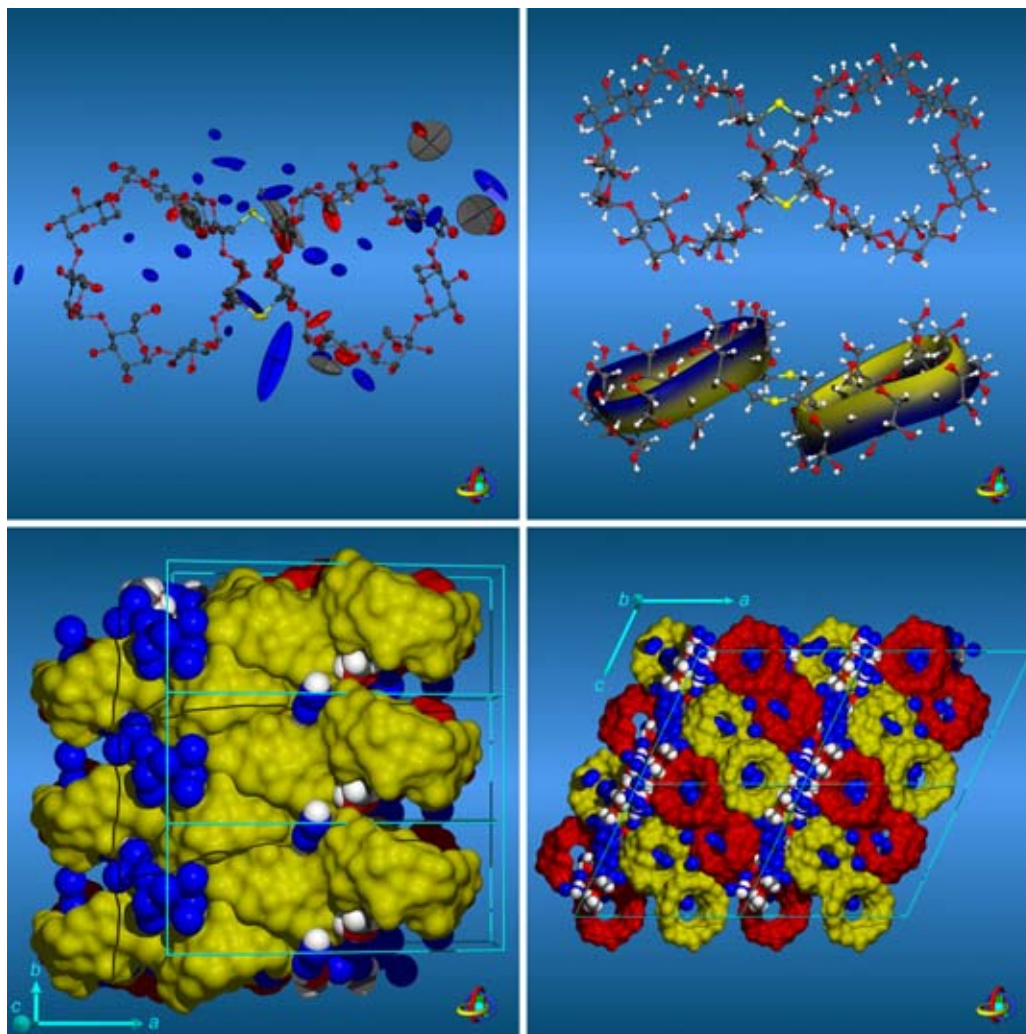


Figure 3. Solid-state structure of $5 \cdot 5\text{MeOH} \cdot 23\text{H}_2\text{O}$. Top left: Molecular geometry and anisotropic 50% probability ellipsoids for the non-hydrogen atoms of the asymmetric unit; for clarity the water oxygen atoms are colored blue. Top right: Front- and side-view ball-and-stick-type models displaying the sulfur linker between the two β -CD units. The ribbon model (the black edge of which corresponds to the side of the CDs carrying the secondary 2- and 3-OH groups, while the yellow rim corresponds to the primary 6- CH_2OH groups) clearly shows the *trans*-relationship between both CD rings. Bottom left: As represented by their yellow contact-surfaces,^[23] the β -CD-dimers are stacked in the crystal lattice in a herringbone-like fashion ($1 \cdot 3 \cdot 1$ unit cells, viewed down the *c*-axis). Bottom right: The stacks of CDs are arranged in layers as indicated by alternating red and yellow surfaces ($2 \cdot 1 \cdot 2$ unit cells, view down the *b*-axis); each β -CD cavity is occupied by four or five water molecules, the rest of the waters of crystallization and the methanol molecules occupy interstitial positions between the macrocycles; water molecules (blue spheres) and methanol are represented as CPK-type solid spheres.

no disorder was observed. The linked CD macrocycles feature almost identical over-all shapes, their backbones being superimposable with an average deviation of only 0.22 Å in their atomic positions (non-hydrogen atoms except for all O6 atoms).

Conclusion

A short and efficient synthesis of a new β -CD dimer has been presented, in which two β -CD units are connected in a head-to-head fashion with a very short sulfur linker. Of the two isomers expected to emerge from the cross-coupling reaction, only the *trans*-type compound was isolated while the *cis*-type compound was not detected. X-ray analysis unequivocally established the *trans*-type linkage of the CD moieties of **5** in a zigzag shape. The molecular geometry of **5** is characterized by

an almost parallel arrangement of the mean ring planes of the two undistorted CD rings fused together through an elongated planar hexagon consisting of the C6^A-S-C6^{A'} and C6^B-S-C6^{B'} fragments within the sulfur linkages. The *trans* dimer opens up the possibility of specifically forming inclusion complexes with potential guest molecules of 1:2 stoichiometry. Moreover, the rather rigid linkage and the “handcuff-like” shape of the dimeric host molecule with two separated cavities may allow included guest molecules and their long-range interactions at well-defined distances to be studied.

Experimental Section

General: β -CD was obtained from the Japan Maize Products Co. Ltd. and used without further purification. 4,6-Dimethoxy-1,3-benzenedisulfonyl chloride was synthesized by chlorosulfonation of 1,3-dimethoxybenzene.^[27]

Pyridine and DMF were dried over 4 Å molecular sieves. Other solvents and chemicals were of reagent grade and used as received from commercial sources. Reversed-phase column chromatography was performed on a Merck prepacked Lobar column (LiChroprep® RP-18, Size B or C). NMR spectra were recorded on a Varian Unity plus 500 spectrometer, and D₂O was used as solvent. Chemical shifts were referenced to acetonitrile (internal standard, $\delta_{\text{H}} = 1.98$ ppm, $\delta_{\text{C}} = 1.70$ ppm). FAB-MS spectra were recorded on a JEOL JMS-HX110 spectrometer.

6^A,6^B-(4,6-dimethoxy-1,3-benzenedisulfonyl)- β -cyclodextrin (1): 4,6-Dimethoxy-1,3-benzenedisulfonyl chloride (2.50 g, 9.23 mmol) was added to a solution of β -CD (6.33 g, 5.58 mmol) in dry pyridine (500 mL). The mixture was stirred at 40 °C for 2.5 h. After the reaction had been quenched by adding water (5 mL), the solvent was removed in vacuo. The residue was taken into 10% aqueous MeOH solution (1 L) and filtered, and the filtrate was then subjected to reversed-phase Lobar column chromatography with gradient elution from 10–40% aqueous methanol (1 L for each). The 20 mL fractions containing the capped CD were combined and evaporated. Lyophilization of the residue afforded the desired product **1** (2.52 g, 32%).

6^A,6^{A'}:6^B,6^{B'}-bis(thia)-bis(6^A,6^B-dideoxy- β -cyclodextrin) (5): KI (3.90 g, 23.5 mmol) was added to a solution of the capped CD **1** (3.19 g, 2.29 mmol) in dry DMF, and the resultant mixture was stirred at 80 °C for 4.5 h. After removal of the solvent in vacuo, the residue was taken into 35% aqueous MeOH solution and filtered. Chromatography of the filtrate on a reversed-phase Lobar column with gradient elution from 10–40% aqueous methanol (1 L for each) gave 6^A,6^B-diiodo- β -CD **2** (2.31 g, 75%).

Alternatively, the capped CD **1** (0.5 g, 0.36 mmol) was treated with thiourea (0.55 g, 7.2 mmol) in DMF at 90 °C for 20 h. The product was precipitated with acetone (0.2 L) and purified by Lobar column chromatography. Eluting the column with a gradient from 100% H₂O–10% aqueous MeOH (1 L for each) yielded the 6^A,6^B-dithiuronium salt **3** (0.44 g, 79%). This (0.15 g, 0.10 mmol) was dissolved in aqueous NaOH solution (0.25 N, 2.5 mL) and stirred at 90 °C for 10 min. The solution was cooled down to RT, and NaBH₄ (25 mg, 0.66 mmol) was added. Ten minutes later, the reaction solution was acidified to pH 3 with 1 N HCl while being cooled with ice-water bath, then acetone (300 mL) was added to precipitate the dithiol **4**. The crude dithiol **4** was dried in vacuo, taken into DMF (6 mL), and filtered. Diiodide **2** (0.15 g, 0.11 mmol) and cesium carbonate (0.13 g, 0.4 mmol) were added to the filtrate. The mixture was degassed, stirred at RT for 66 h under argon, neutralized with 1 N HCl followed by addition of acetone (300 mL) to precipitate the CD species. Chromatography of the precipitate on a reversed-phase Lobar column (gradient elution from 100% H₂O to 40% aqueous MeOH, 1 L for each) gave the pure CD dimer **5** (41 mg, 19% based on engaged dithiuronium salt **3** or 16% based on the capped CD **1**). FAB-MS: m/z : 2266.1 [M^+] (calcd 2266.2 for C₈₄H₁₃₆O₆₆S₂⁺). ¹H and ¹³C NMR are given in Figure 1. Cooling the NMR sample solution (30 mg in 0.6 mL D₂O, CH₃CN as internal standard) to 5 °C yielded single crystals suitable for X-ray diffraction.

Solid-state structure of 5·5MeOH·23H₂O: A suitable single crystal of **5** with dimensions 0.52 × 0.24 × 0.16 mm was sealed in a tube and subjected to X-ray analysis on a Siemens CCD three-circle diffractometer with graphite-monochromated radiation MoK α ($\lambda = 0.71073$ Å) at low temperature $T = 100(2)$ K. The electron density of the solvent in the crystal lattice was approximated through molecules of water and methanol. Analysis of the structure and the hydrogen-bonding network in the crystal lattice yielded 23 additional water molecules and five molecules of methanol (presumably from chromatographic purification) per dimeric β -CD unit. Structure parameters were determined as follows: $M_r = 2840.61$ g mol⁻¹ (C₈₄H₁₃₆O₆₆S₂·5CH₃OH·23H₂O), monoclinic, space group C2, $a = 35.557(2)$, $b = 12.3387(5)$, $c = 31.543(2)$ Å, $\beta = 115.272(4)$, $V = 12514.3(12)$ Å³, $Z = 4$, $\rho = 1.508$ g cm⁻³, $\mu(\text{MoK}\alpha) = 0.167$ mm⁻¹, $F(000) = 5888$, θ range 0.71–25.31°, with limiting indices $-42 \leq h \leq 42$, $-14 \leq k \leq 14$, and $-37 \leq l \leq 37$. Of the 72505 reflections collected 22474 were independent ($R_{\text{int}} = 0.0740$). The structure was solved by direct methods (SHELXS-97)^[28] and successive Fourier synthesis. Refinement (on F^2) was performed by the full-matrix least-squares method with SHELXL-97.^[28] $R(F) = 0.0823$ for 18524 reflections with $I > 2\sigma(I)$, $\omega R(F^2) = 0.2382$ for all 22474 reflections ($\omega = 1/[\sigma^2(F_o^2) + (0.1670P)^2 + 23.4030P]$); in which $P = (F_o^2 + 2F_c^2)/3$. All non-hydrogen atoms (except for one methanol oxygen atom) were refined anisotropically (reflections 22474/parameters 1663/

restraints 6). Hydrogen atoms were considered in calculated positions with the 1.2 U_{eq} value of the corresponding bound atom.

CCDC-190090 contains the supplementary crystallographic data for this paper. These data can be obtained free of charge via www.ccdc.cam.ac.uk/conts/retrieving.html (or from the Cambridge Crystallographic Data Centre, 12 Union Road, Cambridge CB2 1EZ, UK; fax: (+44) 1223-336033; or deposit@ccdc.cam.ac.uk).

Molecular graphics were generated by using the MolArch⁺ program.^[30]

Acknowledgement

The authors are grateful to Prof. F. W. Lichtenthaler and Prof. H. J. Lindner for lucid discussions and to Sabine Foro for collecting the crystallographic data.

- [1] A special issue on cyclodextrins: *Chem. Rev.* **1998**, 98(5).
- [2] I. Tabushi, Y. Kuroda, K. Shimokawa, *J. Am. Chem. Soc.* **1979**, 101, 1614–1615.
- [3] a) K. Fujita, S. Ejima, T. Imoto, *J. Chem. Soc. Chem. Commun.* **1984**, 1277–1278; b) *Chem. Lett.* **1985**, 11–14.
- [4] R. Breslow, N. Greenspoon, T. Guo, R. Zarzycki, *J. Am. Chem. Soc.* **1989**, 111, 8296–8297.
- [5] a) D.-Q. Yuan, Y. Okabe, K. Fujita, *Chin. Chem. Lett.* **1997**, 8, 475–476; b) Y. Ishimaru, T. Masuda, T. Iida, *Tetrahedron Lett.* **1997**, 38, 3743–3744; c) B. Brady, R. Darcy, *Carbohydr. Res.* **1998**, 309, 237–241; d) F. Charbonnier, A. Marsura, I. Pintér, *Tetrahedron Lett.* **1999**, 40, 6581–6583; e) J. Yan, R. Watanabe, M. Yamaguchi, D.-Q. Yuan, K. Fujita, *Tetrahedron Lett.* **1999**, 40, 1513–1514; f) J. Yan, R. Breslow, *Tetrahedron Lett.* **2000**, 41, 2059–2062; g) S.-H. Chiu, D. C. Myles, R. L. Garrell, J. F. Stoddart, *J. Org. Chem.* **2000**, 65, 2792–2796; h) M. R. de Jong, J. F. J. Engbersen, J. Huskens, D. N. Reinhoudt, *Chem. Eur. J.* **2000**, 6, 4034–4040; i) K. J. C. van Bommel, M. R. de Jong, G. A. Metselaar, W. Verboom, J. Huskens, R. Hulst, H. Kooijman, A. L. Spek, D. N. Reinhoudt, *Chem. Eur. J.* **2001**, 7, 3603–3615; j) Y. Liu, Y. Chen, L. Li, G. Huang, C.-C. You, H.-Y. Zhang, T. Wada, Y. Inoue, *J. Org. Chem.* **2001**, 66, 7209–7215; k) Y. Liu, B. Li, C.-C. You, T. Wada, Y. Inoue, *J. Org. Chem.* **2001**, 66, 225–232.
- [6] a) Y. Wang, A. Ueno, F. Toda, *Chem. Lett.* **1994**, 167; b) F. Venema, C. M. Baselier, M. C. Feiters, R. J. M. Nolte, *Tetrahedron Lett.* **1994**, 35, 8661–8664; c) Y. Okabe, M. Yamamura, K. Obe, K. Ohta, M. Kawai, K. Fujita, *J. Chem. Soc. Chem. Commun.* **1995**, 581–582; d) D.-Q. Yuan, K. Fujita, H. Mizushima, M. Yamaguchi, *J. Chem. Soc. Perkin Trans. 1* **1997**, 3135–3136.
- [7] a) M. Luo, W. Chen, D.-Q. Yuan, R. Xie, *Synth. Commun.* **1998**, 28, 3845–3848; b) D. K. Leung, J. H. Atkins, R. Breslow, *Tetrahedron Lett.* **2001**, 42, 6255–6258; c) K. Sasaki, M. Nagasaka, Y. Kuroda, *Chem. Commun.* **2001**.
- [8] a) T. Jiang, M. Li, D. S. Lawrence, *J. Org. Chem.* **1995**, 60, 7293–7297; b) R. Breslow, X. Zhang, R. Xu, M. Maletic, R. Merger, *J. Am. Chem. Soc.* **1996**, 118, 11678–11679.
- [9] R. Breslow, S. Sung, *J. Am. Chem. Soc.* **1990**, 112, 9659–9660.
- [10] a) F. Venema, A. E. Rowan, R. J. M. Nolte, *J. Am. Chem. Soc.* **1996**, 118, 257–258; b) F. Venema, P. Berthault, R. J. M. Nolte, *Chem. Eur. J.* **1998**, 4, 2237–2250.
- [11] a) R. Breslow, B. Zhang, *J. Am. Chem. Soc.* **1992**, 114, 5882–5883; b) R. Breslow, B. Zhang, *J. Am. Chem. Soc.* **1994**, 116, 7893–7894; c) B. Zhang, R. Breslow, *J. Am. Chem. Soc.* **1997**, 119, 1676–1681.
- [12] a) R. Breslow, Z. Yang, R. Ching, G. Trojandt, F. Odobel, *J. Am. Chem. Soc.* **1998**, 120, 3536–3537; b) D. K. Leung, Z. Yang, R. Breslow, *Proc. Natl. Acad. Sci. USA* **2000**, 97, 5050–5053.
- [13] H. Ikeda, Y. Horimoto, M. Nakata, A. Ueno, *Tetrahedron Lett.* **2000**, 41, 6483–6487.
- [14] J. Liu, G. Luo, X. Ren, Y. Mu, Y. Bai, J. Shen, *Biochim. Biophys. Acta* **2000**, 1481, 222–228.
- [15] a) Y. Kuroda, T. Hiroshige, T. Sera, Y. Shiroiwa, H. Tanaka, H. Ogoshi, *J. Am. Chem. Soc.* **1989**, 111, 1921; b) Y. Kuroda, M. Ito, T. Sera, H. Ogoshi, *J. Am. Chem. Soc.* **1993**, 115, 7003–7004.

- [16] a) R. Breslow, Y. Huang, J. Yang, *Proc. Natl. Acad. Sci. USA* **1997**, *94*, 11156–11158; b) J. Yang, R. Breslow, *Angew. Chem.* **2000**, *112*, 2804–2806; *Angew. Chem. Int. Ed.* **2000**, *39*, 2692–2694.
- [17] a) R. R. French, P. Holzer, M. G. Leuenberger, W.-D. Woggon, *Angew. Chem.* **2000**, *112*, 1321–1323; *Angew. Chem. Int. Ed.* **2000**, *39*, 1267–1269; b) R. R. French, W.-D. Woggon, J. Wirz, *Helv. Chim. Acta* **1998**, *81*, 1521–1527.
- [18] D.-Q. Yuan, J.-Z. Lu, M. Atsumi, A. Izuka, M. Kai, K. Fujita, *Chem. Commun.* **2002**, 730–731.
- [19] R. Breslow, S. Halfon, B. Zhang, *Tetrahedron* **1995**, *51*, 377–388.
- [20] a) I. Tabushi, K. Shimokawa, N. Shimizu, H. Shirakata, K. Fujita, *J. Am. Chem. Soc.* **1976**, *98*, 7855–7856; b) I. Tabushi, Y. Kuroda, K. Yokota, L. C. Yuan, *J. Am. Chem. Soc.* **1981**, *103*, 711–712; c) I. Tabushi, K. Yamamura, T. Nabeshima, *J. Am. Chem. Soc.* **1984**, *106*, 5267–5270.
- [21] R. Breslow, J. W. Canary, M. Verney, S. T. Waddell, D. Yang, *J. Am. Chem. Soc.* **1990**, *112*, 5212–5219.
- [22] *Two-Dimensional NMR Spectroscopy* (Eds.: W. R. Croasmun, R. M. K. Carlson), VCH, Weinheim, **1994**.
- [23] a) M. L. Connolly, *J. Appl. Crystallogr.* **1983**, *16*, 548–558; b) M. L. Connolly, *Science* **1983**, *221*, 709–713.
- [24] K. B. Lipkowitz, K. Green, J. A. Yang, *Chirality* **1992**, *4*, 205–215.
- [25] F. W. Lichtenthaler, S. Immel, *Liebigs Ann.* **1996**, 27–37.
- [26] a) D. Cremer, J. A. Pople, *J. Am. Chem. Soc.* **1975**, *97*, 1354–1358; b) G. A. Jeffrey, J. H. Yates, *Carbohydr. Res.* **1979**, *74*, 319–322.
- [27] M. Sekine, J. Matsuzaki, T. Hata, *Tetrahedron* **1985**, *41*, 5279–5288.
- [28] Sheldrick, G. M. *SHELXS-97 and SHELXL-97 Programs for Crystal Structure Solution and Refinement*, University of Göttingen, Germany, **1997**.
- [29] a) F. H. Allen, S. Bellard, M. D. Brice, B. A. Cartwright, A. Doubleday, H. Higgs, T. Hummelink, B. G. Hummelink-Peters, O. Kennard, W. D. S. Motherwell, J. R. Rodgers, D. G. Watson, *Acta Crystallogr. Sect. B* **1979**, *35*, 2331–2339; b) F. H. Allen, O. Kennard, R. Taylor, *Acc. Chem. Res.* **1983**, *16*, 146–153.
- [30] S. Immel, *MolArch⁺, MOLEcular ARCHitecture Modeling Program V7.05*, Technical University of Darmstadt, **2002**.

Received: August 2, 2002

Revised: March 8, 2003 [F4310]